Space Mapping Technique for Electromagnetic Optimization

John W. Bandler, *Fellow, IEEE*, Radoslaw M. Biernacki, *Senior Member, IEEE*, Shao Hua Chen, *Member, IEEE*, Piotr A. Grobelny, and Ronald H. Hemmers, *Student Member, IEEE*

***Abstract*— We offer space mapping (SM), a fundamental new theory to circuit optimization utilizing a parameter space transformation. This technique is demonstrated by the optimization of a microstrip structure for which a convenient analytical/empirical model is assumed to be unavailable. For illustration, we focus upon a three-section microstrip impedance transformer and a double folded stub microstrip filter and explore various design characteristics utilizing an electromagnetic (EM) field simulator. We propose two distinct EM models: coarse for fast computations, and the corresponding fine for a few more accurate and well-targeted simulations. The coarse model, useful when circuit-theoretic models are not readily available, permits rapid exploration of different starting points, solution robustness, local minima, parameter sensitivities, yield-driven design and other design characteristics within a practical time frame. The computationally intensive fine model is used to verify the space-mapped designs obtained exploiting the coarse model, as well as in the SM process itself.**

I. Introduction

We present a new theory and results applicable to circuit optimization with accurate electromagnetic (EM) simulations driven by powerful gradient-based optimizers. We go far beyond the prevailing use of stand alone EM simulators, namely, validation of designs obtained using analytical/empirical circuit models. We embark on the feasibility of efficient, automated EM optimization applicable to arbitrary geometries. Feasibility of performance-driven and yield-driven circuit optimization employing EM simulations has already been shown in previous pioneering works [1], [2]. The main focus of this paper is a fundamental new theory which we call space mapping (SM).

The hierarchy of models to choose from includes: simplified continuous models, detailed continuous models, discrete coarse models, discrete fine models and, ultimately, actual hardware measurements. The continuous or analytical/empirical models usually employ circuit theory whereas the discrete models are based on EM field theory. In general, the circuit-theoretic models are simple and efficient, but may lack the necessary accuracy or have limited validity range. The field-theoretic models are more complex and CPU intensive but can be significantly more accurate. Furthermore, the field-theoretic models are applicable to general geometries. Thus, when deciding on a model, the designer must consider the existence, complexity, accuracy, cost and time associated with each model. Also, different models could be used at different stages of the design process.

In this paper, we concentrate on a mathematical link between the discrete coarse and the discrete fine EM field models. EM simulation time can be significantly reduced if a coarse model is employed. This may decrease the accuracy of EM analysis but qualitative and often quite accurate quantitative information about the behavior of the circuit can be exploited. The coarse model allows us to explore different optimization starting points, solution robustness, local minima, parameter sensitivities and statistics, and other design characteristics within a practical time frame. As design data accumulates we attempt to analytically align the coarse model with the more accurate fine model.

We introduce the SM technique to direct the bulk of CPU intensive optimization to the coarse model while preserving the accuracy and confidence offered by the fine model. The SM optimization technique requires very few fine model simulations in the design process. SM is a general approach and can be used to align other models in the hierarchy. For example, in [3], an advanced application of this concept is described in the design of a high-temperature superconducting quarter-wave parallel coupled-line microstrip filter. There, an EM model is used as the fine model and an analytical/empirical circuit equivalent model is used as the "coarse" model.

To show the benefits of coarse modeling, we carry out nominal optimization of a three-section microstrip impedance transformer [2], [4]. We verify the design with the fine model.

To illustrate the SM technique, we perform SM nominal optimization of a double folded stub microstrip filter [5] using the coarse model and verify the results with the fine model. Encouraged by good consistency of the results we use the coarse model to perform the otherwise very CPU demanding analysis of robustness of our optimized solution. Subsequently, we proceed with SM yield optimization of the filter. For comparison, we perform direct fine model yield optimization. In our work we utilize the OSA90/hope optimization environment [6] with the Empipe [7] interface to the *em* field simulator from Sonnet Software [8].

Manuscript April 8, 1994; revised June 24, 1994. This work was supported in part by Optimization Systems Associates Inc. and in part by the Natural Sciences and Engineering Research Council of Canada under Grants OGP0007239, OGP0042444 and STR0117819.

The authors are with Simulation Optimization Systems Research Laboratory, Department of Electrical and Computer Engineering, McMaster University, Hamilton L8S 4L7, Canada.

J. W. Bandler, R. M. Biernacki, and S. H. Chen are also with Optimization Systems Associates Inc., P.O. Box 8083, Dundas, Ontario L9H 5E7, Canada.

IEEE Log Number 9405426.

In Section II, we explore the theory of our new SM technique. In Section III, we demonstrate the use of coarse modeling and fine model verification in designing a three-section microstrip impedance transformer. Section IV illustrates the SM technique applied to the design of a double folded stub microstrip filter. Sections V and VI contain results of exploiting the coarse model in robustness analysis of minimax design and in SM yield optimization. Finally, Section VII contains our conclusions.

II. Theory

Consider an optimization problem for a given set of design specifications. The behavior of the system may be described by two distinct models, namely, a coarse model and a fine model.

Let us define an l-dimensional vector of fine model parameters as

$$\phi_f = [\phi_{f1}\phi_{f2}\dots\phi_{fl}]^T \tag{1}$$

and a k-dimensional vector of coarse model parameters as

$$\phi_c = [\phi_{c1}\phi_{c2}\dots\phi_{ck}]^T. \tag{2}$$

Also, let $R_f(\phi_f)$ denote the fine model response at ϕ_f. This response is assumed to be accurate but CPU intensive to obtain. Similarly, let $R_c(\phi_c)$ denote the coarse model response at ϕ_c. This response is generally less accurate but faster to compute.

The key idea behind the SM optimization technique is the generation of an appropriate transformation

$$\phi_c = \mathbf{P}(\phi_f) \tag{3}$$

mapping the fine model parameter space to the coarse model parameter space such that

$$\|\mathbf{R}_f(\phi_f) - \mathbf{R}_c(\phi_c)\| \le \epsilon \tag{4}$$

within some local modeling region around the optimal coarse model solution ϕ_c^*, where $\|\cdot\|$ indicates a suitable norm and ϵ is a small positive constant. Though not necessary, it is desirable that $\mathbf{P}$ is invertible. If so, once the transformation (3) is established, the inverse transformation

$$\overline{\phi}_f = \mathbf{P}^{-1}(\phi_c^*) \tag{5}$$

is used to find the fine model solution $\overline{\phi}_f$ which is the image of ϕ_c^* subject to (4).

Finding $\mathbf{P}$ is an iterative process. We begin with a set of fine model base points $\mathbf{B}_f = \{\phi_f^1, \phi_f^2, \dots, \phi_f^m\}$. The initial m base points are selected in the vicinity of a reasonable candidate for the fine model solution. For example, if ϕ_f and ϕ_c consist of the same physical parameters ($k = l$) then the set $\mathbf{B}_f$ can be chosen as $\phi_f^1 = \phi_c^*$ and some local perturbations around ϕ_f^1. Once the set $\mathbf{B}_f$ is chosen, we evaluate the fine model responses $\mathbf{R}_f(\phi_f^i), i = 1, 2, \dots, m$. Next, we find, by parameter extraction, the coarse model set $\mathbf{B}_c = \{\phi_c^1, \phi_c^2, \dots, \phi_c^m\}$ such that (4) holds for each pair of corresponding base points in $\mathbf{B}_f$ and $\mathbf{B}_c$. Using these initial sets, we establish $\mathbf{P}_1$.

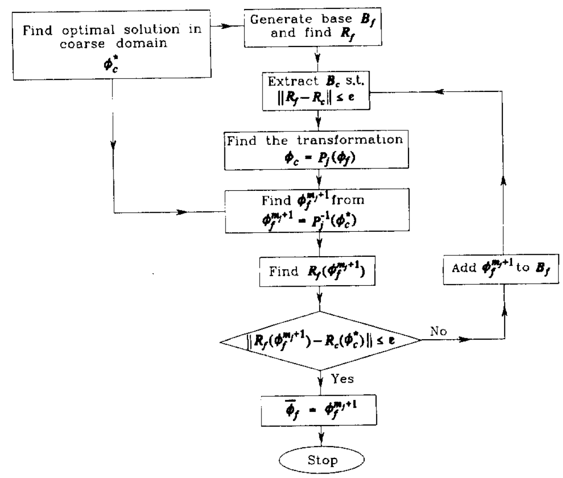

Fig. 1. Flow chart for the space mapping (SM) optimization technique.

At the jth iteration both sets contain m_j base points which are used to establish $\mathbf{P}_j$. To check if $\mathbf{P}_j$ is the desired $\mathbf{P}$, we compute $\phi_f^{m_j+1}$ using the inverse transformation $\mathbf{P}_j^{-1}$

$$\phi_f^{m_j+1} = \mathbf{P}_j^{-1}(\phi_c^*) \tag{6}$$

and evaluate $\mathbf{R}_f(\phi_f^{m_j+1})$. If

$$\|\mathbf{R}_f(\phi_f^{m_j+1}) - \mathbf{R}_c(\phi_c^*)\| \le \epsilon \tag{7}$$

then $\phi_f^{m_j+1}$ is the desired fine model solution $\overline{\phi}_f$ and we have the transformation $\mathbf{P} = \mathbf{P}_j$. If (7) does not hold, we expand $\mathbf{B}_f$ by $\phi_f^{m_j+1}$ and $\mathbf{B}_c$ by $\phi_c^{m_j+1}$ extracted subject to (4). Using the new sets $\mathbf{B}_f$ and $\mathbf{B}_c$, $\mathbf{P}_{j+1}$ is found. This procedure is repeated until (7) holds. Fig. 1 shows a flow chart for this procedure.

We define each of the transformations $\mathbf{P}_j$ as a linear combination of some predefined and fixed fundamental functions

$$f_1(\phi_f), f_2(\phi_f), f_3(\phi_f), \dots, f_n(\phi_f) \tag{8}$$

as

$$\phi_{ci} = \sum_{s=1}^{n} a_{is} f_s(\phi_f) \tag{9}$$

or, in matrix form

$$\phi_c = \mathbf{P}_j(\phi_f) = \mathbf{A}_j f(\phi_f) \tag{10}$$

where $\mathbf{A}_j$ is a $k \times n$ matrix, $f(\phi_f)$ is an n-dimensional vector of the fundamental functions and $m_j \ge n$. Consider the mapping $\mathbf{P}_j$ for all points in the sets $\mathbf{B}_f$ and $\mathbf{B}_c$. We have

$$\left[\phi_c^1\ \phi_c^2 \dots \phi_c^{m_j}\right] = \mathbf{A}_j \left[f(\phi_f^1)\ f(\phi_f^2) \dots f(\phi_f^{m_j})\right]. \tag{11}$$

Define

$$\mathbf{C} = \left[\phi_c^1 \phi_c^2 \dots \phi_c^{m_j}\right]^T \tag{12}$$

and

$$\mathbf{D} = \left[f(\phi_f^1) f(\phi_f^2) \dots f(\phi_f^{m_j})\right]^T. \tag{13}$$

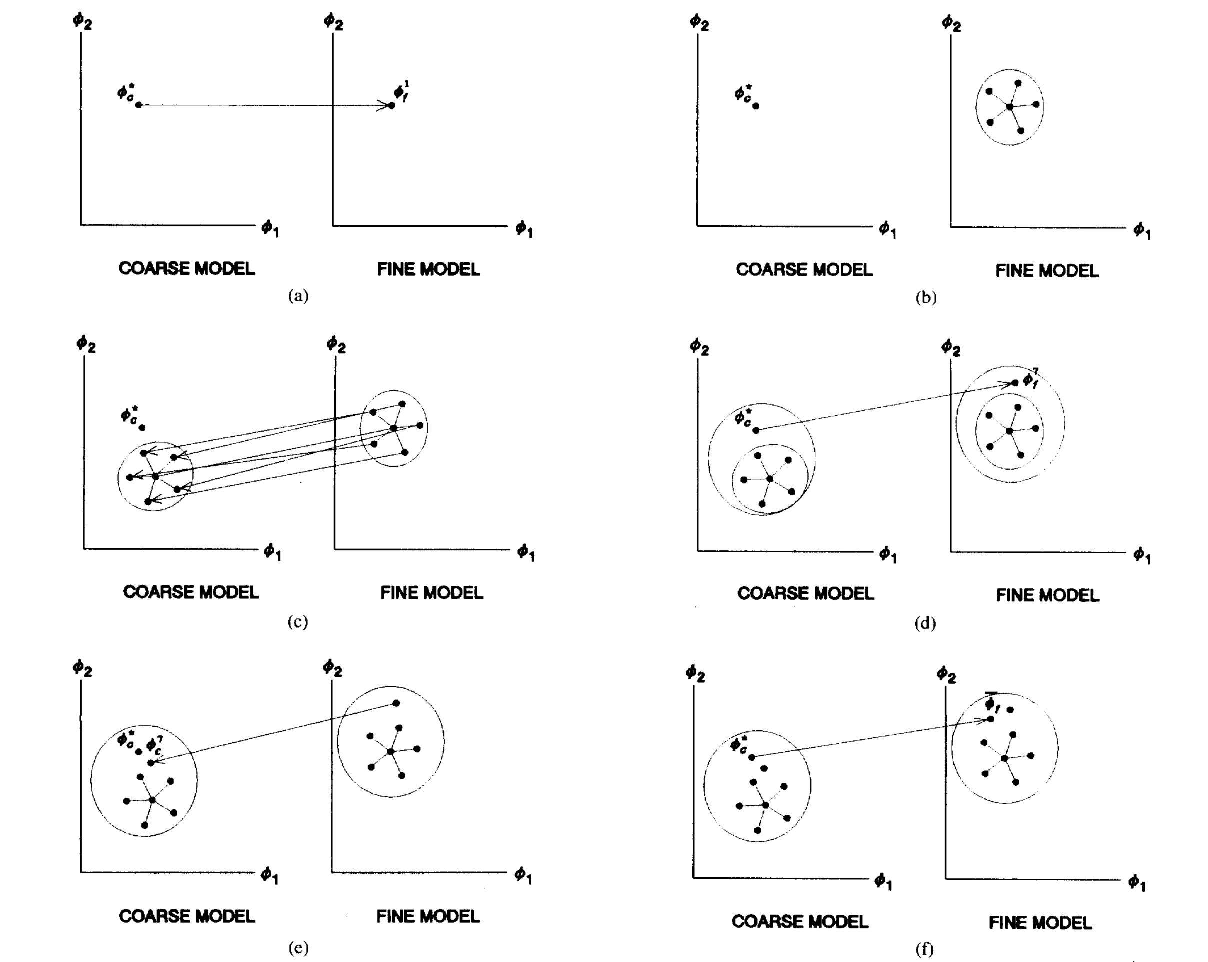

Fig. 2. Illustration of space mapping: (a) setting $\phi_f^1 = \phi_c^*$, (b) generating five base points around ϕ_f^1, (c) performing coarse model parameter extraction to match the fine model responses at all base points, (d) applying the inverse transformation to obtain the fine model point $\phi_f^{m_j+1} = \phi_f^7$, (e) performing coarse model parameter extraction to obtain ϕ_c^7, (f) applying the updated inverse transformation to obtain $\overline{\phi}_f = \phi_f^8$.

Then (11), augmented by some weighting factors defined by an $m_j \times m_j$ diagonal matrix $\mathbf{W}$, where

$$\mathbf{W} = \mathrm{diag}\{w_i\} \tag{14}$$

can be rewritten as

$$\mathbf{W}\mathbf{D}\mathbf{A}_j^T = \mathbf{W}\mathbf{C}. \tag{15}$$

The least-squares solution to this system is

$$\mathbf{A}_j^T = \left(\mathbf{D}^T\mathbf{W}^T\mathbf{W}\mathbf{D}\right)^{-1}\mathbf{D}^T\mathbf{W}^T\mathbf{W}\mathbf{C}. \tag{16}$$

Larger/smaller weighting factors emphasize/deemphasize the influence of the corresponding base points on the SM transformation.

The SM optimization process is illustrated graphically in Fig. 2. We start by setting the first fine model base point ϕ_f^1 to the optimal coarse model solution ϕ_c^*. We then select five additional base points in the vicinity of ϕ_f^1. Parameter extraction is carried out on all six fine model base points to generate the corresponding six coarse model base points. Using these two sets of points, a transformation is found and used to generate the next fine model base point ϕ_f^7. This point does not satisfy condition (7), and so the corresponding coarse model base point ϕ_c^7 is extracted. Using the expanded sets, another fine model point ϕ_f^8 is obtained from the new transformation. This point satisfies condition (7) and thus the transformation is established.

III. Nominal Optimization of a Three-Section Microstrip Transformer

We consider the design of a three-section 3:1 microstrip impedance transformer shown in Fig. 3 [2], [4]. The source and load impedances are 50 and 150 Ω, respectively. The design specifications imposed on the magnitude of the input reflection coefficient are as follows:

$$|S_{11}| \le 0.11 \quad \text{for } 5\text{ GHz} \le f \le 15\text{ GHz}.$$

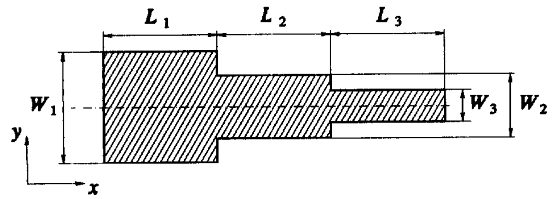

Fig. 3. The three-section 3:1 microstrip impedance transformer.

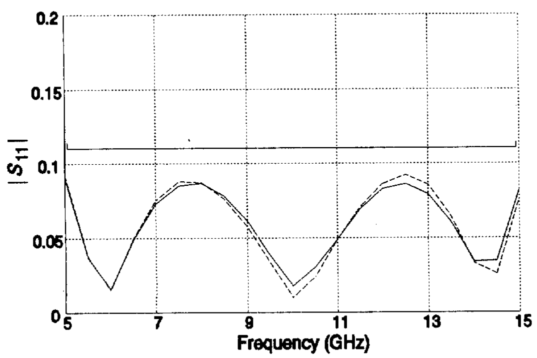

Fig. 4. $|S_{11}|$ of the three-section transformer at the minimax solution as simulated by the coarse model (- - -) and verified by the fine model (—).

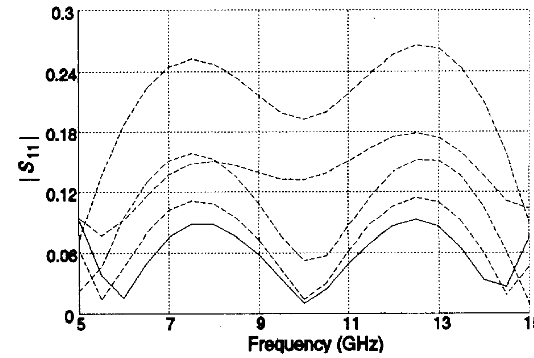

Fig. 5. Coarse model $|S_{11}|$ simulation of the transformer at the off-the-grid minimax solution (—) approximated from four $|S_{11}|$ responses (- - -) obtained at on-the-grid points surrounding the minimax solution.

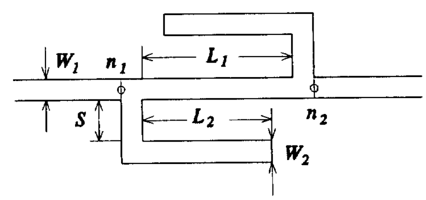

Fig. 6. The double folded stub microstrip filter [5]. n_1 and n_2 indicate the input and output port reference planes, respectively.

The error functions are calculated at frequencies from 5 GHz to 15 GHz with a 0.5 GHz step. The substrate is taken as 0.635 mm thick with relative dielectric constant of 9.7. The widths of the transformer sections, W_1, W_2 and W_3, are considered as optimization variables. The lengths, L_1, L_2 and L_3, are fixed.

We perform minimax design using a coarse model. The x- and y-grid sizes for the numerical EM simulation are chosen as $\Delta x_c = 0.1$ mm and $\Delta y_c = 0.05$ mm. On a Sun SPARCstation 10, 25 CPU minutes are needed to simulate the transformer. This includes automatic response interpolation carried out to accommodate off-the-grid geometries. The maximum of $|S_{11}|$ is decreased from 0.28 at the starting point to 0.09 at the minimax solution. To verify the coarse model design we perform fine model simulation at the coarse model minimax solution. The fine model uses grid sizes of $\Delta x_f = 0.02$ mm and $\Delta y_f = 0.01$ mm. The fine model verification takes about 3 days.

Fig. 4 shows the $|S_{11}|$ responses of the transformer at the coarse model nominal design together with the fine model verification. It can be seen that the coarse model response closely approximates the fine model response. Clearly, in this case, the coarse model can be reliably used in place of the fine model.

Fig. 5 illustrates the interpolation needed to accommodate responses at off-the-grid points. In particular, it shows the coarse model response at the nominal solution together with responses at four on-the-grid points used to approximate the response at the off-the-grid nominal point. In the case of direct fine model optimization this geometrical interpolation would require a significant amount of CPU time.

IV. Coarse Model and SM Optimization of the Double Folded Stub Filter

We optimize the double folded stub filter of Fig. 6 [5]. The design specifications are

$$|S_{21}| \geq -3 \text{ dB} \quad \text{for} \quad f \leq 9.5 \text{ GHz and } f \geq 16.5 \text{ GHz}$$
$$|S_{21}| \leq -30 \text{ dB} \quad \text{for} \quad 12 \text{ GHz} \leq f \leq 14 \text{ GHz}.$$

The error functions are computed at 9 and 15 frequency points taken with a 0.25 GHz step in the stopband and passbands, respectively. The substrate is taken as 5 mil thick with relative dielectric constant of 9.9. The three designable parameters are L_1, L_2, and S. Parameters W_1 and W_2 are fixed at 4.8 mil.

The x- and y-grid sizes for the coarse model simulation are chosen as $\Delta x_c = \Delta y_c = 4.8$ mil. The fine model simulation used to verify the coarse model results uses grid sizes of $\Delta x_f = \Delta y_f = 1.6$ mil. For the coarse model case, the time needed to simulate the filter at a single frequency is about 5 CPU seconds on a Sun SPARCstation 10. This includes automatic response interpolation carried out to accommodate off-the-grid geometries. The corresponding time for the fine model is approximately 70 seconds. The starting point, as well as the coarse model minimax solution are listed in Table I. The $|S_{21}|$ responses of the filter before and after coarse model minimax optimization are shown in Fig. 7 as simulated using the coarse model.

The corresponding fine model response does not satisfy the design specifications. To further refine the solution we applied our new SM optimization technique. The refined SM solution

TABLE I
NOMINAL DESIGN OPTIMIZATION

Parameter (mil)	Before Optimization	Coarse Model Solution	SM Refined Solution
L_1	90.0	91.5	93.7
L_2	80.0	85.7	85.3
S	4.8	4.1	4.6

W_1 and W_2 are kept fixed at 4.8 mil.

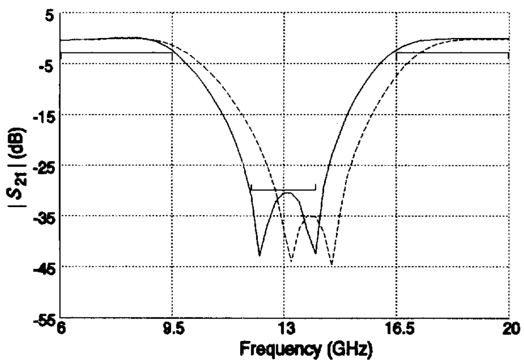

Fig. 7. $|S_{21}|$ of the double folded stub filter before (- - -) and after (—) minimax optimization; both simulated using the coarse model.

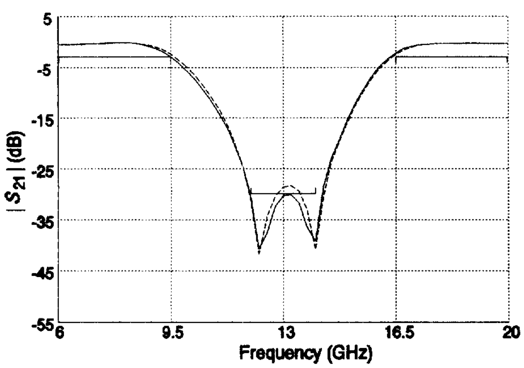

Fig. 8. $|S_{21}|$ of the double folded stub filter at the coarse model minimax solution (- - -) and at the SM refined solution (—); both simulated using the fine model.

is listed in Table I. Fig. 8 shows the $|S_{21}|$ response at the coarse model minimax solution and at the refined SM solution both simulated using the fine model. Fig. 9 shows the $|S_{21}|$ match between the coarse model minimax solution simulated using the coarse model and the SM solution simulated using the fine model. The responses compare very well proving high accuracy of the SM transformation. The main advantage of the SM method is that it requires very few fine model simulations. The SM technique needed only eight fine model simulations to establish a mapping with the resulting match of Fig. 9.

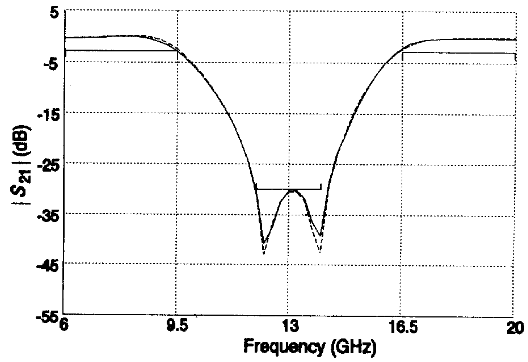

Fig. 9. $|S_{21}|$ of the double folded stub filter at the minimax coarse model solution as simulated using the coarse model (- - -) and at the SM refined solution as simulated using the fine model (—).

TABLE II
FINE MODEL BASE POINTS

Base Point	L_1	L_2	S
ϕ_f^1	91.482	85.735	4.139
ϕ_f^2	96.056	85.735	4.139
ϕ_f^3	91.482	90.021	4.139
ϕ_f^4	91.482	85.735	4.800
ϕ_f^5	86.908	85.735	4.139
ϕ_f^6	86.908	81.448	4.800
ϕ_f^7	93.981	85.324	4.579
ϕ_f^8	93.693	85.314	4.590

All parameter values are in mils. ϕ_f^7 and ϕ_f^8 are generated using subsequent SM transformations. ϕ_f^8 is the SM refined solution $\bar{\phi}_f$.

TABLE III
EXTRACTED COARSE MODEL BASE POINTS

Base Point	L_1	L_2	S
ϕ_c^1	86.392	86.102	4.129
ϕ_c^2	94.694	85.774	3.762
ϕ_c^3	97.242	90.854	2.791
ϕ_c^4	87.462	86.209	4.502
ϕ_c^5	85.092	86.072	3.704
ϕ_c^6	85.002	82.387	3.912
ϕ_c^7	92.096	85.701	4.163

All parameter values are in mils.

In the parameter extraction phase, various optimizers including the ℓ_1, ℓ_2 and the novel Huber [9] optimizer were used to ensure a good match. A subjective criterion based on visual inspection was used to determine the best fit between the corresponding fine and coarse model responses. An automated approach to incorporate (4) in this process is yet to be developed. Tables II and III list the fine and coarse model base points used. Fig. 10 illustrates the parameter extraction process

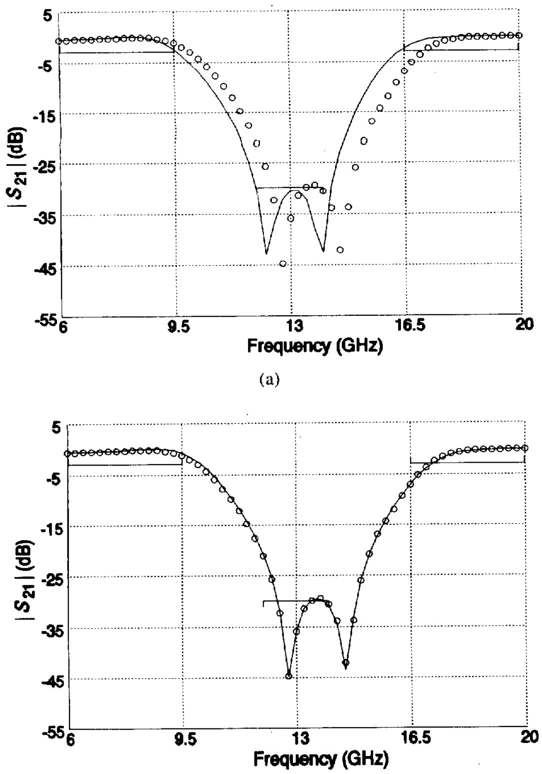

(b)

Fig. 10. $|S_{21}|$ match between the coarse (—) and fine (o) models of the double folded stub filter for the pair of base points ϕ_c^6 and ϕ_f^6 (a) before, and (b) after parameter extraction.

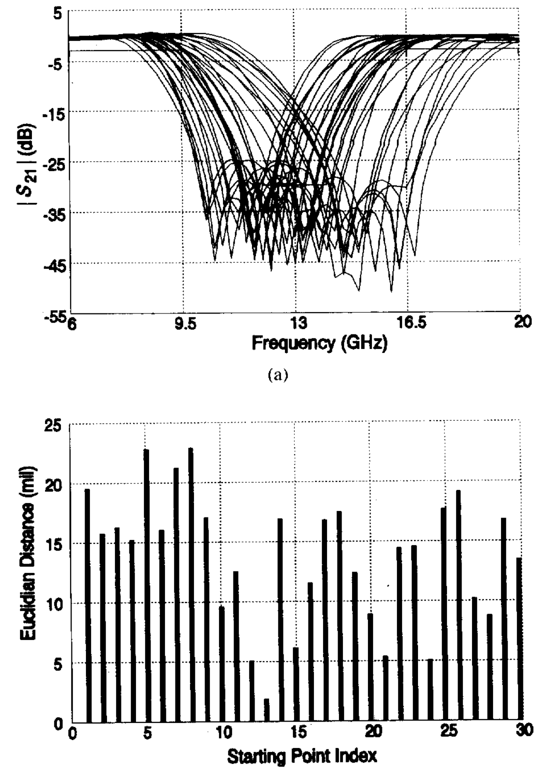

(b)

Fig. 11. (a) $|S_{21}|$ of the double folded stub filter at 30 random starting points, and (b) Euclidian distances between the starting points and the reference minimax solution.

showing the match before and after parameter extraction for a pair of base points.

V. Robustness Analysis of the Nominal Solution

For the double folded stub filter we investigate the robustness of the coarse model nominal solution. The same optimization variables, namely, L_1, L_2 and S, as in the nominal minimax design are selected. W_1 and W_2 are kept fixed. We perform a number of coarse model minimax optimizations, each starting from a different starting point. We use 30 starting points randomly spread around the minimax solution within a $\pm 20\%$ deviation.

Fig. 11(a) plots the $|S_{21}|$ responses for all 30 starting points. The bar chart in Fig. 11(b) depicts the Euclidian distances between the minimax solution and the perturbed starting points. Fig. 12 shows the corresponding diagrams after minimax optimizations. In Fig. 13, we visualize the optimization trajectories taken by the minimax optimizer by showing lines identifying corresponding starting points with optimized solutions for each optimization. These lines are shown for different pairs of designable parameters.

Out of the 30 optimizations, 28 converged to the reference minimax solution. This indicates that the optimized nominal solution is robust. This study has been confirmed using other families of starting points and with other gradient optimizers. A similar analysis with the fine model would be prohibitively time consuming.

VI. Yield Optimization of the Double Folded Stub Filter

For Monte Carlo estimation we assume a uniform distribution with 0.25 mil tolerance on all five geometrical parameters. Yield optimization is performed using the techniques described in [2]. The optimizable parameters are L_1, L_2 and S. W_1 and W_2 are fixed at 4.8 mil. Monte Carlo yield estimated from 250 statistical outcomes using the 4.8 mil coarse model at the coarse model minimax solution is 71%. After coarse model yield optimization using 200 outcomes, the estimated yield is increased to 81%. We then utilize the 1.6 mil fine model to verify the yield at the coarse model nominal and centered solutions. The yield estimated by the fine model is 0% in both cases. This shows the potential pitfalls of relying on coarse-model-only design. Fig. 14(a) shows the $|S_{21}|$ Monte Carlo sweep simulated using the fine model at the coarse model centered solution.

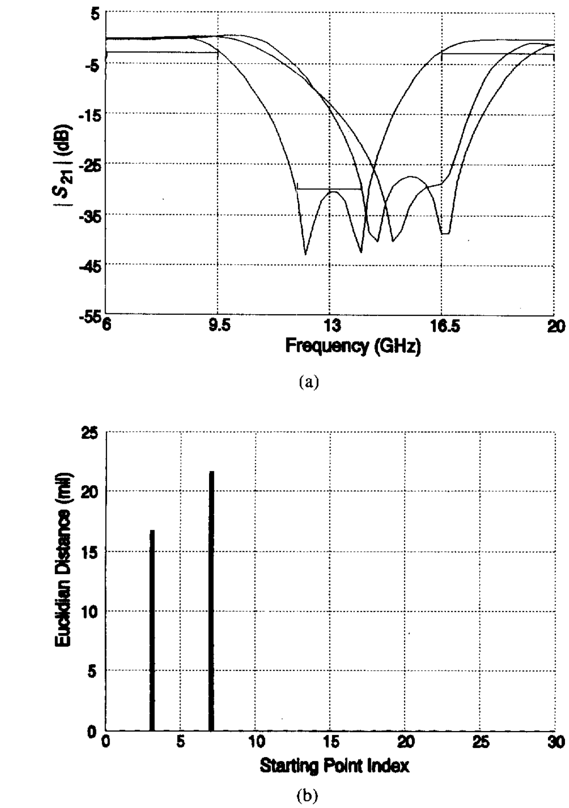

Fig. 12. (a) $|S_{21}|$ of the double folded stub filter at the 30 optimized solutions, and (b) the Euclidian distances between the optimized and the reference minimax solution; note that 28 optimizations converged to the reference minimax solution.

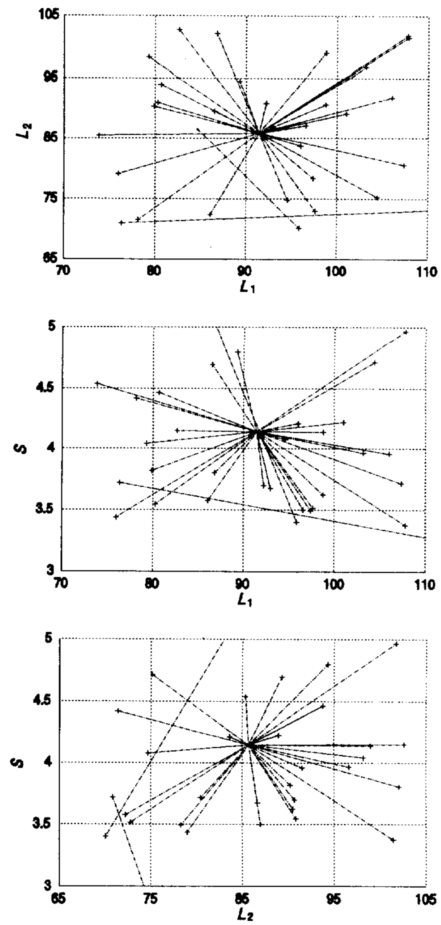

Fig. 13. Visualization of the trajectories taken by the minimax optimizer for each of the randomly generated starting points. Lines connect starting points (+) with the corresponding optimized solutions (·) for different pairs of variables.

Next, we apply the SM concept to yield optimization. The Monte Carlo yield at the starting point (the SM solution) estimated from 250 outcomes and using the fine model is 9%. At each iteration of SM yield optimization, 200 outcomes are generated in the fine model parameter space. Then, the outcomes are mapped, using the forward SM transformation defined by (3) and established in the process of nominal design, into the coarse model parameter space. The mapped outcomes are simulated using the coarse model and the responses are used in the yield optimization. At the solution, the yield is verified using the fine model with 250 outcomes. The yield is increased to 24%. Fig. 14(b) shows the $|S_{21}|$ Monte Carlo sweep simulated using the fine model at the SM centered solution.

The SM yield optimization is compared with direct fine model yield optimization, which produced a comparable yield of 30%. Both solutions are listed in Table IV.

Subsequently, at the SM and fine model centered solutions we perform fine model Monte Carlo analyses with relaxed design specifications. Two cases are considered. For case (a), both the upper and lower specifications are relaxed by 0.5 dB. For case (b), both specifications are relaxed by 1 dB. Yields for the modified specifications are listed in Table V. They are remarkably similar.

TABLE IV
YIELD OPTIMIZATION

Parameter (mil)	Before Yield Optimization	SM Yield Optimization	Fine Model Yield Optimization
L_1	93.7	92.0	91.8
L_2	85.3	85.0	85.1
S	4.6	5.0	4.9
Fine Model Yield	9%	24%	30%

Uniform tolerances of 0.25 mil are assumed on all five geometrical parameters. Yield estimation is based on 250 outcomes. 200 outcomes are used in yield optimization.

VII. CONCLUSIONS

We have presented results involving coarse model nominal design of a three-section microstrip impedance transformer and a double folded stub microstrip filter. For the double folded

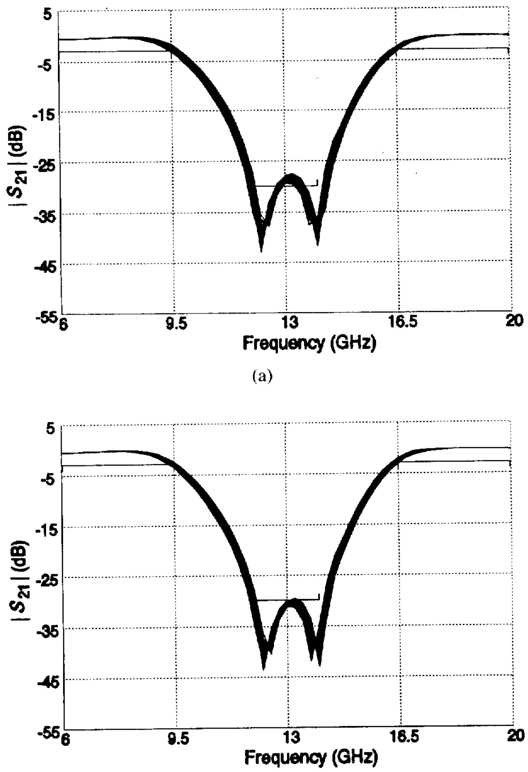

(b)

Fig. 14. $|S_{21}|$ Monte Carlo sweep for the double folded stub filter after (a) coarse model, and (b) SM yield optimization; both simulated using the fine model.

TABLE V
FINE GRID YIELD ESTIMATION FOR RELAXED SPECIFICATIONS

Case	Yield at the Solution of: SM Nominal Design	SM Yield Optimization	Fine Model Yield Optimization
(a)	63%	87%	88%
(b)	81%	97%	96%

Case (a): the lower specification is S_l = -3.5 dB and the upper specification S_u = -29.5 dB.
Case (b): S_l = -4 dB, S_u = -29 dB.

stub filter we have also performed SM nominal optimization and statistical design centering. The statistical design centering was carried out in three different ways: 1) using the coarse model only, 2) using the space mapping transformation, and 3) using the fine model only. In addition, we have analyzed the robustness of the coarse model minimax solution for this filter. In all our experiments, the fine model verifications demonstrate that coarse models can provide useful qualitative and quantitative information about the performance of a circuit within a practical time frame.

We have presented a new theory describing the novel SM optimization technique, a significantly more efficient alternative to traditional optimization. The SM approach exploits the speed of an efficient coarse model and blends it with a few slow but highly accurate fine model evaluations to effectively perform nominal and yield optimization. In this presentation we used EM simulations with different grid sizes for both the coarse and fine models. Coarse grid EM simulation is particularly attractive for structures for which analytical/empirical or circuit-theoretic models are not readily obtainable. In principle, however, the SM technique can align any pair of models from the hierarchy of available models, including hardware measurements. When existing analytical/empirical models are used as the "coarse" model [3], SM revitalizes the wealth and stretches the validity of these models beyond their originally assumed ranges. The SM technique is the key to design with time consuming simulators since it directs the bulk of CPU intensive optimization to the faster coarse models while preserving the accuracy of the fine models. Only a few fine model simulations may be needed in the entire design process.

ACKNOWLEDGMENT

The authors wish to thank Dr. K. Madsen of the Institute of Mathematical Modeling, Technical University of Denmark, Lyngby, Denmark for early discussions with the first author. Dr. J. C. Rautio of Sonnet Software, Inc., Liverpool, NY is thanked for making *em* available for this work.

REFERENCES

[1] J. W. Bandler, R. M. Biernacki, S. H. Chen, D. G. Swanson, Jr., and S. Ye, "Microstrip filter design using direct EM field simulation," *IEEE Trans. Microwave Theory Tech.*, vol. 42, pp. 1353–1359, July 1994.

[2] J. W. Bandler, R. M. Biernacki, S. H. Chen, P. A. Grobelny, and S. Ye, "Yield-driven electromagnetic optimization via multilevel multidimensional models," *IEEE Trans. Microwave Theory Tech.*, vol. 41, 1993, pp. 2269–2278.

[3] J. W. Bandler, R. M. Biernacki, S. H. Chen, P. A. Grobelny, C. Moskowitz, and S. H. Talisa, "Electromagnetic design of high-temperature superconducting microwave filters," *IEEE MTT-S Int. Microwave Symp. Dig.*, San Diego, CA, 1994, pp. 993–996.

[4] J. W. Bandler, R. M. Biernacki, S. H. Chen, and P. A. Grobelny, "A CAD environment for performance and yield driven circuit design employing electromagnetic field simulators," *Proc. Int. Symp. Circuits Syst.*, London, England, vol. 1, 1994, pp. 145–148.

[5] J. C. Rautio, private communication, 1992.

[6] OSA90/hope^{TM}, Optimization Systems Associates Inc., Box 8083, Dundas, Ontario, Canada L9H 5E7, 1994.

[7] *Empipe^{TM}*, Optimization Systems Associates Inc., Dundas, Ontario, Canada L9H 5E7, 1994.

[8] *Em User's Manual*, Sonnet Software, Liverpool, NY 13090–3774, 1993.

[9] J. W. Bandler, S. H. Chen, R. M. Biernacki, L. Gao, K. Madsen, and H. Yu, "Huber optimization of circuits: a robust approach," *IEEE Trans. Microwave Theory Tech.*, vol. 41, 1993, pp. 2279–2287.

John W. Bandler (S'66–M'66–SM'74–F'78), for a photograph and biography, see the July issue of this TRANSACTIONS, page 1358.

Radoslaw M. Biernacki (M'85–SM'86), for a photograph and biography, see the July issue of this TRANSACTIONS, page 1358.

Shao Hua Chen (S'84–M'88), for a photograph and biography, see the July issue of this TRANSACTIONS, page 1359.

Piotr Grobelny was born September 18, 1962. He received the M.S. degree from the Technical University of Wrocław, Wrocław, Poland, in 1987. He is pursuing the Ph.D. at McMaster University, Hamilton, ON, Canada.

From 1987 to 1990, he worked as a Research Assistant in the Machine Building Institute, Technical University of Wrocław, Wrocław, Poland, where he was involved in the development of CAD and CAE software systems. In September 1990, he joined the Simulation Optimization Systems Research Laboratory and the Department of Electrical and Computer Engineering, McMaster University, where he is currently a Teaching Assistant. His research interests are in circuit CAD software design, simulation and optimization techniques, response function modeling techniques, sensitivity analysis, yield optimization, and CAD software integration.

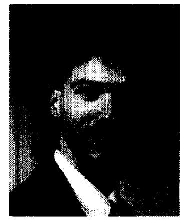

Ronald H. Hemmers (S'91) was born January 25, 1970, in Toronto, ON, Canada. He received the B.Eng. degree in computer engineering from McMaster University, Hamilton, ON, Canada, in 1993. He is pursuing the M.S. degree at the same university.

He joined the Simulation Optimization Systems Research Laboratory and the Department of Electrical and Computer Engineering, McMaster University in May 1993, where he is currently a Teaching Assistant. His research interests include simulation and optimization techniques, design and optimization of microwave circuits, device parameter extraction and statistical analysis and design.